Neutral atoms in ionic lattices: Excited states of KCl:Ag^0

C. Sousa, C. de Graaf, and F. Illas
Departament de Química Física i Centre Especial de Recerca en Química Teòrica, Universitat de Barcelona, Martí i Franquès 1, 08028 Barcelona, Spain

M. T. Barriuso
Departamento de Física Moderna, Facultad de Ciencias, Universidad de Cantabria, 39005 Santander, Spain

J. A. Aramburu and M. Moreno*
Departamento de Ciencias de la Tierra y Física de la Materia Condensada, Facultad de Ciencias, Universidad de Cantabria, 39005 Santander, Spain

(Received 22 December 1999)

The optical-absorption spectrum of a cationic Ag^0 atom in a KCl crystal has been studied theoretically by means of a series of cluster models of increasing size. Excitation energies have been determined by means of a multiconfigurational self-consistent field procedure followed by a second-order perturbation correlation treatment. Moreover results obtained within the density-functional framework are also reported. The calculations confirm the assignment of bands I and IV to transitions of the Ag-5*s* electron into delocalized states with mainly K-4*s*,4*p* character. Bands II and III have been assigned to internal transitions on the Ag atom, which correspond to the atomic Ag-4*d* to Ag-5*s* transition. We also determine the lowest charge transfer (CT) excitation energy and confirm the assignment of band VI to such a transition. The study of the variation of the CT excitation energy with the Ag-Cl distance *R* gives additional support to a large displacement of the Cl ions due to the presence of the Ag^0 impurity. Moreover, from the present results, it is predicted that on passing to NaCl:Ag^0 the CT onset would be out of the optical range while the $5s$-$5p$ transition would undergo a redshift of 0.3 eV. These conclusions, which underline the different character of involved orbitals, are consistent with experimental findings. The existence of a CT transition in the optical range for an atom inside an ionic host is explained by a simple model, which also accounts for the differences with the more common $3d$ systems. The present study sheds also some light on the *R* dependence of the s^2-sp transitions due to s^2 ions like Tl^+.

I. INTRODUCTION

A wide variety of defects and impurities can be formed inside insulating lattices like alkali halides. For instance metal impurities are formed by adding metal halides as AgX, CuX, and TlX to an alkali halide. The positively charged metals (Ag^+, Cu^+, etc.) can occupy alkali cation positions with a typical concentration of one metal cation over 200–10 000 alkali ions. Thereafter, other defects can be created by x irradiation, which causes the formation of free positive and negative charge carriers. The irradiated electrons can be trapped either in halide vacancies to form *F* and *F'* centers, or creating neutral metal centers in cationic positions. On the other hand, the holes can be trapped by the anions originating the so called V_K centers, and also by the cations giving paramagnetic centers (Ag^{2+}, Cu^{2+}).[1]

The formation of neutral atoms like Ag^0,Hg^0,Cu^0,Tl^0 as impurities occupying cationic positions in ionic lattices, is less common, but has been proved to exist through electronic paramagnetic resonance and electron-nuclear double resonance.[2] In the case of Ag^0 in KCl, the hyperfine constant is only about 5% smaller than the corresponding free silver atom value,[2] showing that the electronic configuration of silver is $4d^{10}5s$.[1] Nevertheless, the system cannot be described in terms of a free Ag atom. For instance the optical-absorption spectrum of KCl:Ag^0 shows the presence of an intense band at 6.3 eV while it appears at 5.7 eV for KBr:Ag^0.[3] Based on this shift, this band was tentatively assigned to a $Cl^- \rightarrow Ag^0$ charge-transfer transition.[4] Moreover, an absorption peak appears in the optical spectrum at an energy well below the lowest atomic $5s \rightarrow 5p$ transition.

The whole optical absorption spectrum of KCl:Ag^0 in the violet-ultraviolet (*V*-*UV*) region,[3–6] shows six peaks and for five of them an assignment has been proposed by Moreno.[4,7] Peaks I and VI, the most intense ones, do not depend on the temperature. The intensity of the rest of the bands varies linearly with the temperature denoting that these bands are phonon assisted. Based on these considerations, the first band at 2.92 eV was assigned to a $a_{1g}^* \rightarrow t_{1u}^*$ transition coming from the Ag atomic $5s \rightarrow 5p$ transition. The antibonding a_{1g}^* level was estimated to lie about 2.6–2.9 eV below the bottom of the conduction band, and therefore, it was concluded that the t_{1u}^* level lies within the conduction band. The second and third bands at 4.11 and 4.73 eV were assigned to $e_g^* \rightarrow a_{1g}^*$ and $t_{2g}^* \rightarrow a_{1g}^*$ transitions, respectively. These transitions are not electric dipole allowed, in agreement with the small intensity observed for these bands. Band IV (at 5.35 eV) was related to the silver atomic transition $4d^{10}5s^1 \rightarrow 4d^{10}6s^1$, and finally, the intense band VI at 6.30 eV was interpreted as the first charge-transfer (CT) band and assigned by Moreno to a $t_{1u} \rightarrow a_{1g}^*$ transition.

The latter conclusion is a little surprising, as when isoelectronic cations are considered, the energy of CT transi-

tions decreases as far as the nominal charge increases if the ligand is kept.[8,9] Moreover, at first sight the conclusion appears to be hardly compatible with experimental findings on divalent $3d$ impurities in LiX (X=Cl;Br) lattices.[10,11] In particular, the energy of the first CT transition due to a M^{n+} impurity in LiCl is described (for the case $n=2$) by the following empirical law:

$$E_{\mathrm{CT}}(\mathrm{eV}) = C - I(\mathrm{M}^+) \tag{1}$$

derived by Simonetti and McClure.[11] In this expression, $I(M^+)$ refers to the ionization potential of the free M^+ ion and C is an empirical ''constant'' whose value was found to be 22.4 eV. If we accept that the same law is valid for a M^{n+} impurity with $n \neq 2$ then one would expect $E_{\mathrm{CT}} \approx 20$ eV for KCl:Ag^0 having in mind that $I(Ag^-) = 1.2$ eV.[12] Despite this big discrepancy, previous self-consistent charge extended Hückel (SCCEH) and multiple scattering Xα (MS-Xα) calculations on KCl:Ag^0, supported[13] that the intense band at 6.3 eV can be indeed compatible with a CT assignment. These calculations also showed that the main contribution to the t_{1u}^* level is of K-$4s$,$4p$ character, which supports the assignment of this level to lie within the conduction band. Moreover, they indicate that bands II and III can both arise from $4d^{10}a_{1g}^* - 4d^9(a_{1g}^*)^2$ transitions though the experimental energy difference between both peaks (0.62 eV) can hardly be assigned to the $10Dq$ separation between $e_g^*(4d)$ and $t_{2g}^*(4d)$ one electron orbitals.

To gain a better insight into the rich optical absorption spectrum of KCl:Ag^0, it is necessary to reproduce the main experimental features through more powerful and reliable theoretical methods. To achieve this goal the knowledge of the ground-state equilibrium geometry is crucial as it fully determines the energy of peaks observed in the optical-absorption spectrum. This important prerequisite has been solved in a previous paper by means of total-energy calculations and the analysis of experimental superhyperfine tensor. By both procedures the equilibrium metal-ligand distance R_e is found to be equal to 3.7 Å, a result which concurs with early estimations.[13–15] Moreover it is found that this 18% relaxation of ligands is accompanied by an 8% outwards relaxation of first K^+ ions along $\langle 100 \rangle$ directions.

Having in mind this relevant information, the present paper is devoted to explain the optical absorption spectrum of KCl:Ag^0 by means of reliable methods that include electron correlation in all electronic states. For this goal we first attempt an *ab initio* theoretical study where transition energies are computed at the equilibrium geometry of the ground state (as derived in Ref. 16). To establish the character of the transitions observed in the optical-absorption spectrum, we design various cluster models of increasing size. Excitation energies are computed by constructing highly correlated wave functions based on the multiconfigurational self-consistent field procedure/second-order perturbation correlation treatment (CASSCF/CASPT2) methodology[17,18] implemented in the MOLCAS-4 package.[19] Furthermore, we analyze the dependence of the transition energies with the Ag-Cl distance in order to show the importance of an accurate determination of the relaxation of the lattice around the Ag^0 impurity. This analysis gives additional support for the large outward relaxation of the Cl atoms estimated in previous studies.[13–16,20]

The optical transitions of KCl:Ag^0 have also been calculated using density-functional theory (DFT) methods on clusters of different size. Some results obtained through the MS-Xα method are also reported. It will be shown that these methods quantitatively reproduce the main features of the optical-absorption spectrum due to KCl:Ag^0. The weaker dependence of the computational effort on the size of the system[21] makes DFT certainly interesting to study large systems that are not routinely accessible to handle with traditional quantum chemical techniques. Recent developments in time-dependent DFT (Refs. 22 and 23) may cause this method to become an attractive alternative to study optical properties.

The paper is organized as follows: In the next section we give information about the basis sets, cluster models, embedding schemes, and the computational methods applied in the study of the excited states. In Sec. III, we first calibrate the *ab initio* methods applying them to the free silver atom, thereafter we discuss excitation energies and character of the final states for each separate band observed in the optical-absorption spectrum of KCl:Ag^0. In addition, the variation of the excitation energies with the Ag-Cl distance is discussed in this section. Section III is concluded with a brief discussion of the results reached in the DFT framework on KCl:Ag^0. In Sec. IV we focus on the comparison with other systems. In particular from the R dependence of calculated excitations the optical transition energies for NaCl:Ag^0 are estimated. Finally, we list the conclusions.

II. COMPUTATIONAL INFORMATION

We study the ground and excited states related to the optical transitions mentioned in the introduction in order to extract *ab initio* estimates of excitation energies and to gain insight into the character of these states. For this purpose, we apply a series of cluster models of increasing size. The following six cluster models are studied [see Figs. 1(a)–1(f)]:

- $AgCl_6$,
- $AgCl_6K_{12}$,
- $AgCl_6K_{12}K_6$,
- $AgCl_6K_{12}Cl_8$,
- $AgCl_6K_{12}Cl_8K_6$,
- $AgCl_6K_{12}Cl_8K_2Cl_8K_8$,

where shells of ions around the impurity are progressively added in all three directions except for the largest cluster, for which the 2 K^+ ions in the fourth shell, the 8 Cl^- in the fifth, and the 8 K^+ in the sixth shell are only added in one of the directions giving rise to a noncubic cluster [see Fig. 1(f)]. The Ag^0 valence electrons ($4p^6 4d^{10} 5s^1$) are described with a $(11s,8p,7d)/[4s,4p,4d]$ basis set, while for the Cl^- and K^+ valence electrons ($3s^2$, $3p^6$, and $3p^6$, respectively) we use a $(7s,7p)/[3s,3p]$ basis set. The core electrons of these atoms are represented by Cowan-Griffin relativistic effective core potentials (ECP) which include scalar relativistic effects.[24] For the largest cluster we reduce the basis set of the 8 potassium ions in the outermost shell to $[1s,2p]$ to make the calculations feasible.

To account for the short-range repulsion of the rest of the lattice, all six clusters are surrounded by *ab initio* embedding model potentials (AIEMP).[25,26] The atoms contained in a cube of length $2a$ (being a the lattice parameter of the KCl

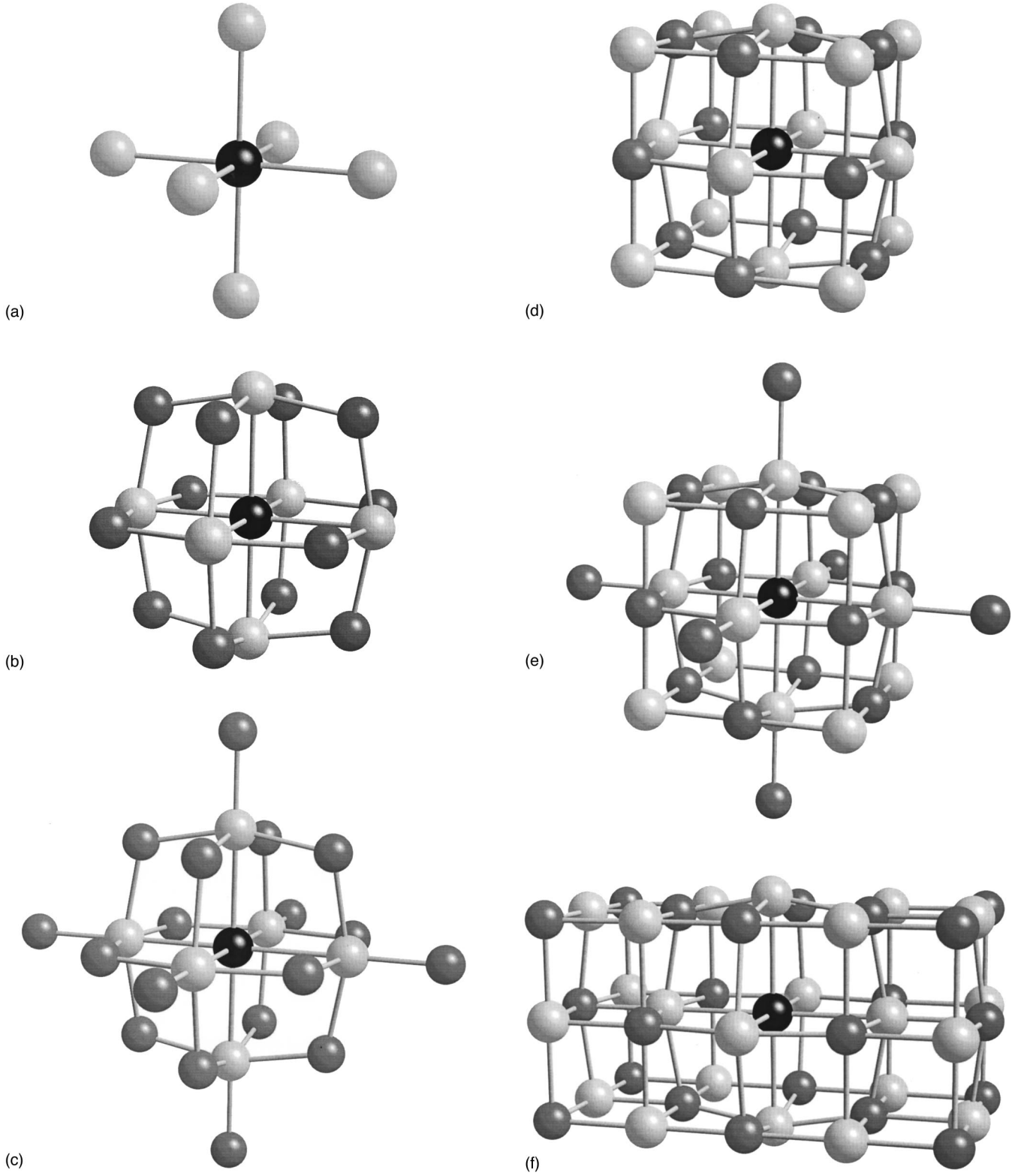

FIG. 1. Cluster models of Ag^0 impurity in KCl at the optimized geometry. Only the atoms explicitly treated are included in the figures. The black sphere represents the Ag^0 impurity, the dark gray spheres refer to K ions, and light gray spheres to Cl ions. From *a* to *f* the following clusters are shown: (a) $AgCl_6$, (b) $AgCl_6K_{12}$, (c) $AgCl_6K_{12}K_6$, (d) $AgCl_6K_{12}Cl_8$, (e) $AgCl_6K_{12}Cl_8K_6$, and (f) $AgCl_6K_{12}Cl_8K_6Cl_8K_8$.

crystal, 6.293 Å) centered in the impurity plus the atoms located at the (3/2,0,0), (3/2,1/2,0), and (3/2,1/2,1/2) unique lattice positions are described as AIEMP's. These model potentials have been optimized to represent the K^+ and Cl^- ions in the pure KCl crystal as described in Ref. 27. Finally, the long-range electrostatic interaction is included in the model by an array of Evjen point charges to complete a cube of $8a$ around the Ag^0 impurity. Although all clusters but the largest one exhibits O_h symmetry, we only exploit the D_{2h} point-group symmetry.

TABLE I. Experimental and theoretical transition energies, TE (in eV), of the Ag atom. The CASSCF wave functions are constructed with an active space that includes 12 orbitals—the 5 Ag (4d) orbitals, 5 Ag (d'), Ag(5s), and Ag(5d)—and 11 electrons. CASPT2 correlates the $4p$, $4d$, and $5s$, electrons. TE average means the weighted average of the spin-orbit splitted components of the ^2D and ^2P states.

	Experiment			Theory	
Configuration	State	TE	TE average	State	CASSCF	CASPT2
$4d^{10}5p^1$	$^2P_{1/2}$	3.66	3.74	^2P	3.68	3.79
	$^2P_{3/2}$	3.78				
$4d^9 5s^2$	$^2D_{5/2}$	3.75	3.97	^2D	4.31	4.00
	$^2D_{3/2}$	4.30				

Excitation energies are estimated as vertical transitions from the optimized ground-state geometry. This geometry has been determined from a restricted open-shell Hartree-Fock calculation for a $AgCl_6K_6$ cluster embedded in AIEMP's and point charges. Because of the large outward relaxation, both the Ag-Cl and Cl-K distances along the three axes have been relaxed. The resulting Ag-Cl distance is 3.707 Å, i.e., an outward relaxation of about 20% comparing to the ideal KCl structure. The optimized Cl-K distance is 2.995 Å, which is only 5% smaller than the ideal Cl-K distance in the KCl crystal. Further details concerning the geometry relaxation can be found in Ref. 16. The rest of the atoms of the clusters, the AIEMP's, and the point charges are fixed at the lattice positions of the KCl crystal.

Multireference wave functions for the states considered are constructed in a CASSCF calculation with an active space containing 11 electrons distributed in all possible ways over 11 orbitals. For all states, we include the five Ag-4d orbitals and a correlating set of five virtual orbitals, usually referred to as Ag-4d'. As has been shown before, this ensures a correct treatment of the large dynamical electron correlation effects in the TM d shell, whereas a perturbational treatment tends to overestimate these correlation effects.[28–31] Note that this is especially important for transitions in which the number of d-electrons changes. For the ground state (a^2A_{1g}), the ^2E_g, the $^2T_{2g}$, and the b^2A_{1g} states, associated to bands II, III, and IV, respectively, we add an orbital of a_{1g} symmetry. For the two $^2T_{1u}$ states related to bands I and VI, the eleventh orbital is of t_{1u} symmetry. Remaining, mostly dynamical, electron correlation effects are included by second-order perturbation theory, CASPT2, in which all valence electrons are correlated. In this perturbational treatment the CASSCF wave function is taken as a zeroth-order wave function. The character of the open shell orbital of the excited states is studied by Mulliken population analysis (MPA). Although it is well known that it has its limitations, this analysis gives a reasonable qualitative insight into the character of the orbitals.

DFT calculations have been performed with the Amsterdam density functional code[32,33] using the local density approximation exchange-correlation functional. Triple zeta basis sets (quality IV) are employed to describe the valence electrons, whereas the core electrons are kept frozen. Results are reported for the 39-atom cluster, $AgCl_6K_{12}Cl_8K_6Cl_6^{2-}$ described in the previous paper.[16] The details of the MS-Xα calculations for the 81-atom cluster, $AgCl_6K_{12}Cl_8K_6Cl_2K_{24}^{4+}$, are also given there.

III. RESULTS AND DISCUSSION

A. Free silver atom

Before attempting the study of the optical spectra of the silver impurity in KCl, we calculate the transition energies for a free silver atom to calibrate the computational approach. The Ag atom is described with the ECP and basis set mentioned before in the computational information. CASSCF wave functions for the ground- and lowest-excited states are constructed by distributing 11 electrons over 12 orbitals (Ag-4d, 4d', 5s, and 5p). CASPT2 accounts for remaining electron correlation. Table I lists the CASSCF/CASPT2 excitation energies of the ^2P (coming from a $4d^{10}5p^1$ configuration) and ^2D (arising from a $4d^9 5s^2$ configuration) excited states with respect to the ^2S ($4d^{10}5s^1$) ground state. A direct comparison with experimental excitation energies cannot be made because of the large spin-orbit splitting present in the silver atom (0.12 eV for the ^2P state and 0.55 eV for the ^2D). Therefore, results are compared with a weighted average of the spin-orbit splitted components of the ^2D and ^2P states. Table I shows that our CASPT2 excitation energies are within 0.05 eV of these weighted averages. This indicates that, except for spin-orbit effects, the computational approach (ECP, basis set and CASSCF/CASPT2 method) is well calibrated and can be used in the system of interest, KCl:Ag^0. Note that CASPT2 lowers the excitation energy for the ^2D state, while a small increase is observed for the ^2P state. The CASSCF wave functions already include the major part of the electron correlation effects caused by the Ag-4d electrons, and hence the stabilization of the ^2D state is caused by the differential electron correlation effects of the 5s electrons treated by CASPT2. The slight destabilization of the transition to the ^2P state must be ascribed to slightly larger electron correlation effects in the 5s than in the 5p orbital.

B. CASSCF/CASPT2 approach to the optical spectrum of KCl:Ag^0

KCl presents a face-centered-cubic structure where each ion is surrounded by six nearest neighbors in a local octahedral symmetry. The Ag^0 impurity substitutes a K^+ ion and the crystal field splits the Ag-4d orbitals into two sets of

TABLE II. CASSCF and CASPT2 excitation energies (in eV) relative to the $^2A_{1g}$ ground state for different cluster models using a Ag-Cl distance of 3.707 Å and a Cl-K distance of 2.995 Å.

State		$AgCl_6$	$AgCl_6K_{12}$	$AgCl_6K_{12}K_6$	$AgCl_6K_{12}Cl_8$	$AgCl_6K_{12}Cl_8K_6$	$AgCl_6K_{12}Cl_8K_2Cl_8K_8$	Exp.
$^2T_{1u}$	CASSCF	3.77	3.61	3.60	3.52	3.53	3.44	2.92
	CASPT2	3.82	3.64	3.65	3.54	3.56		(band I)
^2E_g	CASSCF	4.72	4.75	4.74	4.74	4.74	4.74	4.11
	CASPT2	4.22	4.18	4.15	4.15	4.13		(band II)
$^2T_{2g}$	CASSCF	4.78	4.80	4.80	4.79	4.79	4.80	4.73
	CASPT2	4.29	4.25	4.22	4.22	4.20		(band III)
b^2A_{1g}	CASSCF	13.47	7.58		5.95		5.59	5.35
	CASPT2	13.48	7.52		5.75			(band IV)
$^2T_{1u}$	CASSCF	12.37	8.13		8.12		8.13	6.29
(CT)	CASPT2	10.71	6.46		6.38			(band VI)

orbitals of $e_g(d_{x^2-y^2}, d_{3z^2-r^2})$ and $t_{2g}(d_{xy}, d_{yz}, d_{xz})$ symmetry. In this section we study the five assigned bands observed in the spectrum using the cluster models and computational approach commented before. Table II summarizes the excitation energies of the different bands obtained with the six different clusters. In order to analyze the optical spectrum of the Ag^0 impurity in KCl we study and interpret each band separately.

1. Band I at 2.92 eV

The band appearing at 2.92 eV has been assigned to a $a_{1g}^* \rightarrow t_{1u}^*$ transition, which in the free Ag atom corresponds to a $5s \rightarrow 5p$ transition. The entry in Table II for the $^2T_{1u}$ state shows the variation of the excitation energies on going from the smallest cluster, $AgCl_6$, to the larger ones. The excitation energy of the $^2A_{1g} \rightarrow {}^2T_{1u}$ transition decreases with increasing the cluster size. This reduction is accompanied by a delocalization of the open shell orbital in the excited state for the larger clusters. Indeed, this orbital has a strong Ag-$5p$ character for the smallest $AgCl_6$ cluster and extends over the K ions as the size of the cluster increases. The inclusion of the 12 K surrounding the basic $AgCl_6$ cluster already leads to a significant delocalization; the Ag-p character of the open shell orbital of the excited state drops to 77% and the excitation energy decreases about 0.2 eV. Adding six K in the $\langle 1,0,0 \rangle$ directions to the $AgCl_6K_{12}$ cluster, does not significantly affect the excitation energy and the character of the open shell orbital. Instead, inclusion of the next shell of 8 Cl ions causes a stabilization of 0.1 eV and the open shell orbital now has an important contribution ($\sim$31%) of the K-$4s$,$4p$ orbitals. The fact that this delocalization does not occur in the $AgCl_6K_{12}$ cluster indicates that the Cl ions surrounding the K need to be included explicitly in the cluster and that the description of these ions with bare AIEMP's introduces a too strong repulsion that prevents the population of the K-$4s$ and $4p$ orbitals in the $AgCl_6K_{12}$ cluster.

The next entry in Table II ($AgCl_6K_{12}Cl_8K_6$) shows again that incorporation of six K in the $\langle 1,0,0 \rangle$ directions to the $AgCl_6K_{12}Cl_8$ cluster does not change the general image of the transition unless the surrounding Cl^- ions are explicitly included in the cluster. However, this leads to a cluster of unmanageable size if the cluster is extended in all three directions. From the previous clusters, we observe that the orbitals of the K^+ ions located at the (1/2,1/2,0) and (1/2,0,1/2) positions are more populated than those at the (0,1/2,1/2) in agreement with the $t_{1u}(x)$ symmetry of the open shell orbital. Therefore, we extend the $AgCl_6K_{12}Cl_8$ cluster with the $2\,K^+$ ions at the ($\pm$1,0,0) positions and all Cl^- and K^+ nearest neighbors in the same yz plane. This large cluster is referred to as $AgCl_6K_{12}Cl_8K_2Cl_8K_8$ [see Fig. 1(f)] and performing *ab initio* calculations with such a cluster is at the limit of present day computational resources. For this reason, only CASSCF calculations has been performed. However, CASPT2 hardly affects the excitation energies; as can be seen in Table II, the effect is never larger than 0.05 eV. With the largest cluster we find a further delocalization of the open shell orbital over the K^+ ions in the second, fourth, and sixth shell surrounding the impurity and a further decrease of the excitation energy to 3.44 eV, slowly approaching the experimental value of 2.92 eV. The contribution of the Ag-p orbital to the open shell orbital further decreases to approximately 55%.

In summary, the final state connected to the $^2A_{1g} \rightarrow {}^2T_{1u}$ transition is as delocalized as the size of the cluster allows, hence, to have a correct description and an accurate excitation energy of this state, much larger cluster models are needed. Nevertheless, our calculations confirm the delocalized character of this state as a transition into the conduction band of predominantly K-$4s$ and $4p$ character as proposed by Cabria *et al.*[13,20] The delocalized character of the final state explains the lower-excitation energy compared to the corresponding transition in the free atom. The effect of spin-orbit coupling on the transition energy is estimated to be very small. Spin-orbit coupling splits the corresponding atomic transition by 0.1 eV (see Table I), but for the KCl:Ag^0 system, the splitting is expected to be smaller because of the delocalized character of the $^2T_{1u}$ state.

2. Bands II and III at 4.10 and 4.73 eV

Bands II and III in the absorption spectrum have been assigned to $e_g^* \rightarrow a_{1g}^*$ and $t_{2g}^* \rightarrow a_{1g}^*$ transitions, respectively. SCCEH and MS-Xα calculations performed by Cabria *et al.*[13,20] showed that the e_g^* and t_{2g}^* orbitals involved in such transitions, have almost pure Ag-$4d$ character while the a_{1g}^* orbital can be considered as a Ag-$5s$ orbital.

As for the previous band, Table II shows the excitation energies of the $^2A_{1g} \rightarrow {}^2E_g$ and $^2A_{1g} \rightarrow {}^2T_{2g}$ transitions at the

CASSCF (11/11) and CASPT2 level. In the first place, we observe that the excitations energies at a given level of calculation hardly change with increasing cluster size. This illustrates that the excitations are rather local and MPA shows that the excited state open shell orbital indeed has a strong Ag-4d character. It is well known that transitions involving d electrons in transition-metal compounds are very localized and can be accurately described with relative small cluster models.[34–37] As in the free Ag atom, CASPT2 lowers the CASSCF excitation energies, but does not affect the ^2E_g-$^2T_{2g}$ splitting. Moreover, the effect of the dynamical electron correlation on the excitation energies does not change from cluster to cluster; a constant lowering of ~0.5 eV is observed.

Second, the splitting between the ^2E_g and $^2T_{2g}$ states is very small, only 0.07 eV, whereas the experimental separation between bands II and III is 0.62 eV. The difference between experiment and the calculated value must be ascribed to the lack of spin-orbit coupling effects in our calculations. However, these effects can readily be estimated from the free atom because of the very localized character of the transitions. Table I shows a $^2D_{3/2}$-$^2D_{5/2}$ separation of 0.55 eV, which is almost identical to the splitting of bands II and III for KCl:Ag^0. Therefore, we conclude that the separation between bands II and III is mainly due to spin-orbit effects while crystal-field effects are much less important. To properly describe the final states of bands II and III, calculations that explicitly include spin-orbit coupling are indispensable. Nevertheless, our calculations corroborate the assignment of these bands to transitions in which an electron is transferred from the Ag-4d shell to an orbital with mainly Ag-5s character.

3. Band IV at 5.35 eV

The calculated excitation energy connected to the $a^2A_{1g} \rightarrow b^2A_{1g}$ transition, which in an isolated atom corresponds to a $5s \rightarrow 6s$ transition, rapidly reduces as the size of the cluster increases (see Table II). The excitation energy decreases almost 6 eV on going from the smallest $AgCl_6$ cluster to the next one with the 12 K^+ next neighbors included. Transition energies for the $AgCl_6K_{12}K_6$ cluster have not been calculated since the calculations for the previous three bands clearly indicate that inclusion of the six K^+ in the $\langle 1,0,0 \rangle$ directions does not significantly influence the excitation energies. The same holds for the $AgCl_6K_{12}Cl_8K_6$ cluster, which gives similar results as the $AgCl_6K_{12}Cl_8$ cluster model. For the latter cluster, excitation energies are about 2 eV smaller than for the $AgCl_6K_{12}$ cluster and 0.4 eV larger than the one obtained for the largest cluster studied, $AgCl_6K_{12}Cl_8K_2Cl_8K_8$. This indicates that the excitation energy seems to rapidly converge with the cluster size and tends to the experimental value of 5.35 eV.

Again, for the largest cluster, no CASPT2 estimate can be given because of the very large computational demands of such a calculation. However, the results of the other clusters indicate that electron correlation tends to lower the CASSCF value by a small amount, and therefore, we expect that CASPT2 will lower the CASSCF excitation energy for the largest cluster, 5.59 eV, approaching the experimental value even more. Concerning the nature of the open shell orbital in the excited state, MPA shows that this orbital extends all over the cluster. The highly delocalized character means that this orbital belongs to the conduction band of the crystal. Hence, it is not appropriate to relate the open shell orbital in the final state to a 6s-like atomic orbital. Spin-orbit effects for this transition are not important since only unpaired electrons of s character are involved.

4. Band VI at 6.3 eV

Band VI is the last band observed in the optical-absorption spectrum and carries large intensity. It has been assigned to a charge transfer (CT) transition from a t_{1u}Cl-3p orbital to a a_{1g}^* orbital with strong Ag-5s character.[4,13] At first sight, the appearance of local CT transitions at such low energies might be surprising because the Ag impurity changes from a neutral state to a negatively charged state, whereas a positively charged oxidation state is more common for silver.

Excitation energies of this transition obtained for different clusters are reported in Table II [see entry $^2T_{1u}$(CT)]. As for the previous band, only the cluster models, which introduce new effects, are taken into account. In all clusters the open shell of the excited state, $^2T_{1u}$, has a strong Cl-3p character and the $^2A_{1g} \rightarrow {}^2T_{1u}$ transition is ascribed to a local charge-transfer transition. The excitation energy for the smallest cluster is very high, larger than 10 eV. Obviously, such a small cluster cannot account for an excitation in which a hole is formed on the edge of the cluster. The ions in the direct cluster environment are described with model potentials that do not allow these ions to respond to the changes in the charge distribution between Ag and Cl. This artifact seems to be largely removed in the next cluster that includes the 12 K ions surrounding the Cl ions; the excitation energy experiences an important lowering of about 4 eV. The fact that the excitation energy does not change anymore for the larger clusters considered shows that the polarization of the lattice in response to the CT transition is not as long ranged as for ionization processes. Two reasons can be given to rationalize this observation. In the first place, the transfer of an electron from the ligand-p shell to the Ag-5s orbital is accompanied by a redistribution of the density in the closed-shell orbitals. This causes the hole created on the ligands to be effectively screened and therefore the net transfer of charge is smaller than one. For the transition studied here, the net transfer estimated by MPA is ~0.5 electrons. The second reason for the rather short-ranged character of the lattice relaxation can be found in the fact that electron reorganization occurs within a local region. This means that the atoms located further away from the impurity do not experience large changes in the Coulomb potential due to a local CT transition.

Note that the effect of CASPT2 is much larger than for any of the other states considered. The large stabilization of the CT state by CASPT2 has been observed before by Geleijns *et al.*[38] in the study of the local charge transfer processes in NiO. Two effects contribute to the differential electron correlation. The first one is caused by the different Ag-s and Cl-p occupations in the ground and excited state, which tends to stabilize the state with higher s occupation, as has been shown by Sousa *et al.* in the study of the copper halide molecules.[39] The second effect is the recuperation of the orbital relaxation effects.[35,40–42] In the CASSCF wave function of the $^2T_{1u}$(CT) state, an electron is removed from a molecu-

TABLE III. CASPT2 excitation energies (in eV) relative to the $^2A_{1q}$ ground state as function of the Ag^0-Cl distance, R (in Å), for the $AgCl_6K_{12}Cl_8$ cluster. The Ag-K^4 distance is 6.70 Å.

	R			
State	3.146	3.427	3.707	3.800
$^2T_{1u}$	2.71	3.27	3.54	3.58
^2E_g	4.70	4.35	4.15	4.12
$^2T_{2g}$	4.91	4.46	4.22	4.17
b^2A_{1g}	2.61	4.39	5.75	6.10
$^2T_{1u}$(CT)	7.40	7.25	6.38	6.10

lar orbital that is a linear combination of two Cl atomic orbitals. This implies that only part of the orbital relaxation due to the removal of an electron is included in this wave function. CASPT2 has the complete orbital relaxation included up to first order and this causes a further stabilization of the charge-transfer state.

The calculated excitation energy for the CT state is converged with the cluster size. We observe that this transition is genuinely local and can be accurately described with a rather small cluster. The excitation energy is computed to be 6.4 eV, which compares very well with the experimental transition energy of band VI, 6.3 eV. Spin-orbit effects are relatively unimportant as the open shell orbital in the excited state is highly localized on the Cl atom. The atomic spin-orbit splitting for Cl is only 0.1 eV, and hence, it is not expected that the $^2T_{1u}$(CT) state is significantly affected by spin-orbit coupling effects.

5. Influence of the Ag^0-Cl distance on the excitation energies

It is well known that various spectroscopic properties strongly depend on the metal-ligand distance in transition-metal compounds. By studying the dependence of the excitation energies on the local geometry around the Ag^0 impurity, further insight into the electronic structure of the KCl:Ag^0 system can be obtained. This dependence is especially relevant for the present case, since the size of the outward relaxation of the Cl ions due to the presence of the Ag^0 atom is not definitely settled. The excitation energies of the transitions discussed before are calculated at four different Ag-Cl distances using a cluster that accurately describes the electronic states involved in the transitions, namely, the $AgCl_6K_{12}Cl_8$ model. Beside the optimized distance, we consider distances of 3.146 Å corresponding to the K-Cl distance in the pure crystal, a distance of 3.427 Å, which is the minimum of the potential-energy surface varying only the Ag-Cl distance, and finally, we also apply a Ag-Cl distance of 3.8 Å, slightly larger than the optimized value. In all these cases the $6\,K^+$ ions at the axis neighboring the Cl ions are placed at their optimized position as described in the computational information.

Table III, which lists the CASPT2 results, shows that the excitation energies of the delocalized states ($^2T_{1u}$ and b^2A_{1g}) increase with the Ag-Cl distance. This is not surprising as the delocalization, which causes a stabilization of the excited state, is facilitated at smaller distances. The tendency for the localized states [^2E_g, $^2T_{2g}$, and $^2T_{1u}$(CT)] is the opposite; with increasing distance the excitation energies diminishes. The effect of the ligand field on the ^2E_g and $^2T_{2g}$ states decreases with the distance, which explains the trend of the transition energies for these two states towards the atomic value. On the other hand, the explanation of the variation for the $^2T_{1u}$(CT) state is less obvious. This behavior has been previously observed for many octahedral TM compounds and has been rationalized by a more pronounced destabilization of the one-electron levels associated with the metal than those associated with the ligand when the metal-ligand distance decreases.[43,44]

The dependence of the CT transition energy with the distance gives us an additional way to approximately estimate the Ag-Cl distance. The other bands are less suitable for such an analysis since they are either delocalized or lack the effect of spin-orbit coupling. Table III shows that the calculated CT transition energy only coincides with the experimental value when the outward relaxation of the Cl ions surrounding the silver impurity is of the order of 20%, in excellent agreement with previous work.[13–16]

C. DFT approach to the optical spectrum of KCl:Ag^0

Representative DFT and MS-Xα results on optical transitions due to KCl:Ag^0 are summarized in Table IV. It can be seen that the main experimental features are also qualitatively reproduced by DFT and MS-Xα calculations, although the agreement with experiment is not as good as for the CASSCF/CASPT2 method. It is worth noting that in the present case, DFT results lead to an underestimation of 2.2 eV of the CT energy. The results collected in Table IV have been derived maintaining all ions (except the Cl^- ligands) at the equilibrium positions for the perfect KCl lattice. It is worth noting that the energies of optical transitions are little dependent on the positions of these ions. For instance, the energy of the charge-transfer transition experiences a variation less than 1% when the first K^+ ions along ⟨100⟩ directions are placed at the equilibrium geometry found for the Ag^0 center.

In principle two allowed CT transitions can be observed in the spectrum of a s^1 ion in an octahedral site: First, a transition in which an electron is transferred from a $t_{1u}(\pi)$ orbital with dominant ligand-p_π character, and second, from a $t_{1u}(\sigma)$ orbital, mainly built from p_σ ligand orbitals. It has been shown[45,46] that for transitions like the two $t_{1u}\rightarrow a_{1g}^*$ transitions of KCl:Ag^0 the oscillator strength directly depends on the amount of σ admixture in the ligand orbital. For KCl:Ag^0 the present DFT calculations indicate that the σ admixture for the so-called $t_{1u}(\sigma)$ orbital is about nine times bigger than for $t_{1u}(\pi)$. This situation is quite different to

TABLE IV. LDA and MS-Xα transition energies (in eV) at two different Ag-Cl distances. LDA calculations are performed with a 39-atoms cluster whereas MS-Xα results are reported for a 81-ions cluster. The results shown have been calculated placing all ions (except Cl^- ligands) at the equilibrium positions corresponding to the perfect KCl lattice.

	Theory				Expt.
	$R=3.60$ Å		$R=3.70$ Å		
Transition	MS-Xα	LDA	MS-Xα	LDA	
$a_{1g}^*\rightarrow t_{1u}^*$ (Ag-5p)	3.47	3.89	3.62	4.00	2.92
$e_g^*\rightarrow a_{1g}^*$	4.09	3.26	4.24	3.08	4.11
$t_{2g}^*\rightarrow a_{1g}^*$	4.16	3.17	4.29	2.99	4.73
$t_{1u}(\pi)\rightarrow a_{1g}^*$	5.54	4.04	5.43	3.90	
$t_{1u}(\sigma)\rightarrow a_{1g}^*$	5.88	4.19	5.83	4.04	6.29

that found for $CuCl_4^{2-}$, TlC_6^{4-}, or CrF_6^{3-} units embedded in insulating lattices.[45–47] Such a difference can be ascribed to the relative closeness of the 5p orbital of Ag^0 in the present case, which tends to destroy the significant σ-π hybridization in the t_{1u} orbitals found for $CuCl_4^{2-}$, $TlCl_6^{4-}$, or CrF_6^{3-} units.[46]

The results collected in Table IV indicate that the separation between the two CT transitions is around 0.25 eV, which is comparable to the experimental bandwidth.[48] Despite this fact it is expected that the CT peak observed experimentally arises essentially from the $t_{1u}(\sigma)\rightarrow a_{1g}^*$ transition, because of the small oscillator strength of the $t_{1u}(\pi)\rightarrow a_{1g}^*$ CT transition.

Within the DFT framework the electronic relaxation in the $^2T_{1u}(\sigma)$ excited state has also been analyzed. When the ground-state Kohn-Sham orbitals are used, the CT energy is found to be 0.9 eV higher than when relaxed orbitals are employed. At the same time the total charge on central ion decreases by 0.4e once the electron density is allowed to relax. The resulting net charge transfer is equal to 0.35e. This result is similar to that reached through *ab initio* calculations (Sec. III B) and indicates that electronic relaxation effects for the $^2T_{1u}(\sigma)$ excited CT state of KCl:Ag^0 are smaller than those for open shell 3d ions.[45,49–51]

IV. COMPARISON WITH 3d AND OTHER S^1 SYSTEMS

Though the present calculations strongly support the existence of a CT transition in the optical range for KCl:Ag^0 it is also necessary to understand why the widely used empirical law [Eq. (1)] reported by Simonetti and McClure[11] is no longer valid for the present case. The main origin for such a discrepancy can be well accounted for through a simple model. Let us consider a highly ionic MX_6 species (X=halide) embedded in an insulating lattice. The work required for extracting an electron from a ligand level and placing it at the zero energy level can be approximated by

$$W(\mathrm{X})=E(\mathrm{X})+U_c(\mathrm{X})-U_R(\mathrm{X}), \tag{2}$$

where $U_c(\mathrm{X})=(e^2/R)[z_M-3.3z_X]$ reflects the electrostatic interaction of an electron on a ligand with all other ions of the complex, $U_R(\mathrm{X})$ accounts for the interaction with the rest of the ions in the lattice and $E(\mathrm{X})$ means the electron affinity of free X atom. z_M and z_X are the formal charges of the metal and the ligand, and R the M-X distance.

Assuming that the metal cation M^{n+} becomes $M^{(n-1)+}$ after the CT process, the work required to carry an electron from the cation to the zero energy level can be approximated by

$$W(\mathrm{M})=I(\mathrm{M}^{(n-1)+})-U_c(\mathrm{M})-U_R(\mathrm{M}). \tag{3}$$

In this expression $U_c(\mathrm{M})=6z_Xe^2/R$ and $I(\mathrm{M}^{(n-1)+})$ is the ionization potential of free $M^{(n-1)+}$ ion. Equation (3) does however not consider all important facts in a CT process because (i) antibonding electrons spend some time on the ligands and (ii) once a hole is created on the ligands, there is a flow of electronic charge from the metal to the ligands through the closed-shell orbitals. These effects lead to an effective work $W(\mathrm{M})$ that is higher than that described by Eq. (3).

If all this kind of contributions to E_CT are considered through an additional term denoted as U_R, E_CT can be deduced by subtracting Eq. (2) and Eq. (3):

$$E_\mathrm{CT}=E(\mathrm{X})+Q-U_r-I(\mathrm{M}^{(n-1)+}), \tag{4}$$

with $Q=U_c(\mathrm{X})+U_c(\mathrm{M})$. If the complex is mainly ionic in its ground state one would expect that $U_r>0$. To derive Eq. (4) it has been assumed that $U_R(\mathrm{M})=U_R(\mathrm{X})$. This condition is well fulfilled for substitutional impurities in cubic lattices (see Refs. 52–54 for further discussion). When expression (4) is compared to Eq. (1) it turns out that the empirical term C is equal to $E(\mathrm{X})+Q-U_r$. For divalent impurities in LiCl $R\approx 2.5$ Å; $E(\mathrm{Cl})=3.6$ eV, and $Q\approx 27$ eV. The comparison with $C=22.4$ eV derived from experiments indicates that U_r is indeed positive and equal to ≈ 8 eV. However, it is important to note that this analysis also shows that the term C in Eq. (1) cannot be considered as a constant when the nature of the impurity is changed. On passing from divalent 3d ions to Ag^0 not only changes R significantly, but also the z_M involved in $U_c(\mathrm{X})$. Putting now $R=3.7$ Å and $z_\mathrm{M}=0$ in Eqs. (2)–(4) it turns out that Q becomes equal to 10 eV for KCl:Ag^0 and hence C is much smaller than 22.4 eV. With this reduced C, the existence of a CT transition in the optical range can now reasonably be understood.

As previously pointed out[43,45] the term dQ/dR appears to be a main factor controlling the R dependence of a CT transition. In the present case, $dQ/dR\approx -2.8$ eV/Å, which is comparable to the dE_CT/dR values derived from Table III. From this value, it is now possible to estimate E_CT for

NaCl:Ag^0. Assuming $R_e = 3.37$ Å, as previously reported,[4] the energy of the first allowed CT transition in NaCl:Ag^0 is predicted to be 7.2 eV, i.e., a blueshift of 0.9 eV with respect to what is measured in KCl:Ag^0. Therefore the first allowed CT transition in NaCl:Ag^0 would not be located in the more accessible optical range but in the vacuum UV region. A similar conclusion is obtained from the DFT results of Table IV though in this case $dE_{CT}/dR \approx -1.5$ eV/Å. Further experimental work is necessary to check this relevant prediction.

Experimentally the Ag-$5s \rightarrow 5p$ transition in NaCl:Ag^0 is found within the optical range the corresponding energy being equal to 2.65 eV.[2] When compared to KCl:Ag^0 the redshift undergone by that transition can reasonably be accounted for by the results contained in Tables III and IV. These results indicate that the Ag-$5s \rightarrow 5p$ transition experiences a redshift when R decreases, a behavior that is just the opposite to that found for a CT transition. Taking $dE/dR \approx 0.9$ eV/Å for this transition from Table III, one expects a value of approximately 2.60 eV for NaCl:Ag^0.

Finally, we discuss the Ag-$5s \rightarrow 6s$ transition appearing at 5.16 eV in NaCl:Ag^0 (Refs. 2 and 3) and thus suffering a redshift of 0.19 eV with respect to KCl:Ag^0. Although for transitions from a_{1g}^* to higher one-electron levels, the results gathered in Table III predict a redshift when R decreases, it is also derived $dE(5s\text{-}6s)/dR \approx 3.5$ eV/Å, implying a redshift close to 1 eV. This discrepancy indicates that in order to describe the $^2A_{1g}$ excited state larger clusters are needed.

The present results can also be compared with recent experimental data and MS-Xα calculations on the $6s^1$ ion Tl^{2+} in different alkali halides.[47] It turns out that when R decreases, the CT transitions undergo a blueshift whereas the Tl-$6s \rightarrow 6p$ transition experiences a redshift. This general trend has to be related to the different character of the involved one electron orbitals in $n_M s^1$ impurities ($n_M = 5$ for Ag^0, $n_M = 6$ for Tl^{2+}) placed in insulating lattices. In a CT transition, the electron jumps from a localized orbital on ligands to an orbital with mainly $n_M s^1$ character, which is localized to a reasonable extent on the central ion. When R decreases the increase of electrostatic repulsion on an electron placed in a_{1g}^* increases the energy of this level and thus favors the increase of the CT transition energy. By contrast, the t_{1u}^* orbital with mainly $n_M p$ character is much less localized on the central ion than a_{1g}^*. Therefore the increase of electrostatic repulsion for decreasing R is stronger on a_{1g}^* than on t_{1u}^*, which explains the observed redshift. Although this qualitative trend is followed by both impurities, the sensitivity to R changes is of course different in both cases. For instance, for the $t_{1u}(\sigma) \rightarrow a_{1g}^*$ transition of $TlCl_6^{4-}$, MS-Xα calculations[47] lead to $dE_{CT}/dR = 7.9$ eV/Å. The significant increase of dE_{CT}/dR on passing from KCl:Ag^0 to $TlCl_6^{4-}$ can be understood by the fact that for $TlCl_6^{4-}$ R_e has been estimated to be 2.8 Å and the nominal charge of Tl^{2+} is not zero but $z_M = 2$.

The present results are helpful to understand relevant experimental facts coming from s^2 ions in insulating lattices. For instance the energy of $n_M s^2 \rightarrow n_M sp$ optical transitions due to ions like Tl^+ or Sn^{2+} is also found to increase slightly along the series NaCl-KCl-RbCl.[55]

V. CONCLUSIONS

In this paper, we have presented *ab initio* cluster model calculations in order to study and analyze the optical absorption spectrum of a Ag^0 impurity in a KCl lattice. We have constructed CASSCF wave functions for ground and excited states involved in the transitions and remaining dynamical electron correlation has been accounted for by second-order perturbation theory by means of CASPT2. This approach, together with the basis sets and ECP's applied, have been proven to be adequate to give accurate estimates of the transition energies of the free silver atom.

Five bands in the optical spectrum of the Ag^0:KCl system have been studied in detail and characterized. The first band corresponds to a transition to a delocalized state with mainly K-4*s*,4*p* character. In our cluster calculations the final state is as delocalized as the size of the cluster allows and the excitation energy slowly approaches the experimental value of 2.92 eV as the cluster size increases. Band IV shows a similar delocalized character and convergence of the excitation energy towards the experimental value of 5.35 eV. Therefore, states of KCl:Ag^0 coming from $5p$ and $6s$ states of free Ag^0 are in fact resonant states. Bands II and III have been confirmed to arise from transitions localized on the Ag atom in which an electron is excited from the Ag-$4d$ to the Ag-$5s$ orbital. Spin-orbit coupling have been found to be essential in order to explain the right splitting between the two bands; crystal-field effects are of minor importance.

The origin of the small band called *V* and peaked at 5.6 eV is not clarified through the present paper. Despite the $5s \rightarrow 6p$ transition of free silver atom placed at 6.0 eV,[4] this can hardly be the origin of band *V* as its intensity is temperature dependent.[3] This fact strongly suggests that band V is a parity forbidden transition as it happens for bands II, III, and IV.[3]

Finally, we have confirmed the previous tentative assignment of Moreno[4] of band VI to a local CT transition. The calculated transition energy of 6.4 eV is converged with the cluster size and in good agreement with the absorption band observed at 6.3 eV. From the dependence of the CT excitation energy with the distance, we have given additional support to the outward displacement of 20% of the Cl ions surrounding the Ag^0 impurity, as proposed in previous studies[13–15] and in the preceding paper.[16] A model has been proposed to explain the surprisingly low energy of the CT transition. In spite of the very simple nature, the model serves to understand trends in excitation energies in a variety of impurities in ionic insulators.

ACKNOWLEDGMENTS

We thank Dr. Ria Broer of the University of Groningen for stimulating discussions. The work has been financed by Spanish ''Ministerio de Educación y Ciencia'' under CICyT projects PB98-1216-CO2-01 and PB98-0190. Part of the computer time was provided by the ''Center de Supercomputació de Catalunya,'' C^4-CESCA, through a research grant from the University of Barcelona. C. de G. would like to thank the European Community for financial support.

*Corresponding author. Email: morenom@ccaix3.unican.es

[1] A. M. Stoneham, *Theory of Defects in Solids; Electronic Structure of Defects in Insulators and Semiconductors* (Oxford University Press, Oxford, 1996).
[2] S. V. Nistor, D. Schoemaker, and I. Ursu, Phys. Status Solidi B **185**, 9 (1994).
[3] M. Saidoh and N. Itoh, J. Phys. Soc. Jpn. **35**, 1122 (1973).
[4] M. Moreno, J. Phys. C **13**, 6641 (1980).
[5] C. J. Delbecq, W. Hayes, M. C. M. O'Brien, and P. H. Yuster, Proc. R. Soc. London, Ser. A **271**, 243 (1963).
[6] M. Saidoh, N. Itoh, and M. Ikeya, J. Phys. Soc. Jpn. **25**, 1197 (1968).
[7] M. Moreno, J. Phys. C **12**, I921 (1979).
[8] C. K. Jorgensen, *Solid State Physics* (Academic, New York, 1962), Vol. 13, pp. 375.
[9] C. K. Jorgensen, Prog. Inorg. Chem. **12**, 101 (1970).
[10] S. Hirako and R. Onaka, J. Phys. Soc. Jpn. **51**, 1255 (1982).
[11] J. Simonetti and D. S. McClure, J. Chem. Phys. **71**, 793 (1979).
[12] T. Koga, H. Tatewaki, and A. Thakkar, J. Chem. Phys. **100**, 8140 (1994).
[13] I. Cabria, M. T. Barriuso, J. A. Aramburu, and M. Moreno, Int. J. Quantum Chem. **61**, 627 (1997).
[14] M. T. Barriuso and M. Moreno, Phys. Rev. B **26**, 2271 (1982).
[15] M. Moreno, J. A. Aramburu, and M. T. Barriuso, Phys. Lett. A **87**, 307 (1982).
[16] J. A. Aramburu, M. Moreno, I. Cabria, M. T. Barriuso, C. Sousa, C. de Graaf, and F. Illas (unpublished).
[17] K. Andersson, P.-Å. Malmqvist, B. O. Roos, A. J. Sadlej, and K. Wolinski, J. Phys. Chem. **94**, 5483 (1990).
[18] K. Andersson, P.-Å. Malmqvist, and B. O. Roos, J. Chem. Phys. **96**, 1218 (1992).
[19] K. Andersson, M. R. A. Blomberg, M. P. Fülscher, G. Karlström, R. Lindh, P.-Å. Malmqvist, P. Neogrády, J. Olsen, B. O. Roos, A. J. Sadlej, M. Schütz, L. Seijo, L. Serrano-Andrés, P. E. M. Siegbahn, and P.-O. Widmark, MOLCAS, Version 4, University of Lund, Lund, 1997.
[20] I. Cabria, M. T. Barriuso, J. A. Aramburu, and M. Moreno, Mater. Sci. Forum **239–241**, 171 (1997).
[21] W. Kohn, Phys. Rev. Lett. **76**, 3168 (1996).
[22] E. K. U. Gross, J. F. Dobson, and M. Petersilka, *Density Functional Theory* (Springer-Verlag, Heidelberg, 1996).
[23] M. E. Casida, C. Jamorski, K. C. Casida, and D. R. Salahub, J. Chem. Phys. **108**, 4439 (1998).
[24] Z. Barandiarán and L. Seijo, Can. J. Chem. **70**, 409 (1992).
[25] Z. Barandiarán and L. Seijo, J. Chem. Phys. **89**, 5739 (1988).
[26] L. Seijo and Z. Barandiarán, *Computational Chemistry: Reviews of Current Trends* (World Scientific, Singapore, 1999) Vol. 4.
[27] L. Seijo and Z. Barandiarán, J. Chem. Phys. **94**, 8158 (1991).
[28] B. H. Botch, T. H. Dunning Jr., and J. F. Harrison, J. Chem. Phys. **75**, 3466 (1981).
[29] K. Andersson and B. O. Roos, Chem. Phys. Lett. **191**, 507 (1992).
[30] B. O. Roos, in *New Challenges in Computational Quantum Chemistry*, edited by R. Broer, P. J. C. Aerts, and P. S. Bagus (Groningen, Netherlands, 1994), pp. 12.
[31] K. Pierloot, E. Tsokos, and B. O. Roos, Chem. Phys. Lett. **214**, 583 (1993).
[32] P. Belanzoni, E. J. Baerends, S. van Asselt, and P. B. Langewen, J. Phys. Chem. **99**, 13 094 (1995).
[33] G. te Velde and E. J. Baerends, J. Comput. Phys. **99**, 84 (1992).
[34] A. Fujimori and F. Minami, Phys. Rev. B **30**, 957 (1984).
[35] G. J. M. Janssen and W. C. Nieuwpoort, Phys. Rev. B **38**, 3449 (1988).
[36] L. Pueyo, V. Luaña, M. Flórez, E. Francisco, J. M. Recio, and M. Bermejo, Rev. Solid State Sci. **5**, 137 (1991).
[37] C. de Graaf, R. Broer, and W. C. Nieuwpoort, Chem. Phys. **208**, 35 (1996).
[38] M. Geleijns, C. de Graaf, R. Broer, and W. C. Nieuwpoort, Surf. Sci. **421**, 106 (1999).
[39] C. Sousa, W. A. de Jong, R. Broer, and W. C. Nieuwpoort, Mol. Phys. **92**, 677 (1997).
[40] H. Ågren, P. S. Bagus, and B. O. Roos, Chem. Phys. Lett. **82**, 505 (1981).
[41] R. Broer and W. C. Nieuwpoort, Chem. Phys. **54**, 291 (1981).
[42] R. Broer and W. C. Nieuwpoort, Theor. Chim. Acta **73**, 405 (1988).
[43] J. A. Aramburu, M. Moreno, and M. T. Barriuso, J. Phys.: Condens. Matter **8**, 6901 (1996).
[44] K. Wissing, M. T. Barriuso, J. A. Aramburu, and M. Moreno, J. Chem. Phys. **111**, 10 217 (1999).
[45] J. A. Aramburu, M. Moreno, K. Doclo, C. Daul, and M. T. Barriuso, J. Chem. Phys. **110**, 1497 (1999).
[46] M. T. Barriuso, J. A. Aramburu, C. Daul, and M. Moreno, Int. J. Quantum Chem. **61**, 563 (1999).
[47] I. Cabria, M. Moreno, J. A. Aramburu, M. T. Barriuso, U. Rogulis, and J. M. Spaeth, J. Phys.: Condens. Matter **10**, 6481 (1998).
[48] B. Villacampa, R. Cases, V. M. Orera, and R. Alcalá, J. Phys. Chem. Solids **55**, 263 (1994).
[49] T. Ziegler, A. Rauk, and E. J. Baerends, Theor. Chim. Acta **43**, 261 (1977).
[50] A. C. Stuckl, C. A. Daul, and H. U. Güdel, J. Chem. Phys. **107**, 4606 (1997).
[51] S. Veliah, R. Pandey, and S. Marshall, Modell. Simul. Mater. Sci. Eng. **2**, 933 (1994).
[52] S. Sugano and R. G. Shulmann, Phys. Rev. **130**, 517 (1963).
[53] K. Pierloot, E. van Praet, and L. G. Vanquickenborne, J. Chem. Phys. **96**, 4163 (1992).
[54] J. A. Aramburu and M. Moreno, Phys. Rev. B **56**, 604 (1997).
[55] P. W. Jacobs, J. Phys. Chem. Solids **52**, 35 (1991).